# Nanocomposites Based on Collagen and Na-Montmorillonite Modified with Bioactive Substances

**CATALINA GABRIELA POTARNICHE[1], ZINA VULUGA[1]*, CONSTANTIN RADOVICI[1], SEVER SERBAN[1], DUMITRU MIRCEA VULUGA[2], MARIUS GHIUREA[1], VIOLETA PURCAR[1], VIORICA TRANDAFIR[3], DANA IORDĂCHESCU[4], MĂDĂLINA GEORGIANA ALBU[3]**

[1]National Research and Developement Institute for Chemistry and Petrochemistry-ICECHIM, 202 Splaiul Independentei, 060021, Bucharest, Romania

[2]Centre for Organic Chemistry "C. D. Neniţescu" of Romanian Academy, 202B Splaiul Independentei, 060023, Bucharest, Romania

[3]National Research and Development Institute for Textile and Leather, Division Leather and Footwear Research Institute, 93 Ion Minculescu Str., 031215, Bucharest, Romania

[4]University of Bucharest - Centre for Research in Biochemistry and Molecular Biology, 6 Dinu Vintila Str., 021102, Bucharest, Romania

*Collagene-based nanocomposite membrane films were obtained by dispersing nanohybrides formed by modifying a layered silicate with quebracho and methylene blue in a collagen-gel matrix. TGA and XRD analyses proved the intercalation of active substances between the silicate layers. Thermal stability of the binary nanohybrides decreases with the increase of active substance content. Nanocomposites showed an improved thermal stability compared to collagen. Modifying the silicate with active substances influences the hydrophilicity of final nanocomposite by reducing the water vapour adsorption. Although the methylene blue is a disinfectant, it influences negatively the growth and development of the fibroblasts hence it is inappropriate for use in case of an open lesion. Quebracho is biocompatible and has a biostimulating effect on the growth and development of the fibroblasts, bioactive films thus obtained being good antiseptic and regenerating patches.*

*Keywords: nanocomposites, montmorillonite, collagen, methylene blue, quebracho*

Recent works [1, 2] showed that in order to use collagen for biomedicine and maintaining some effects (biostimulating of cell metabolism, osteoinductor, osteoconductor), modifications in the structure and composition of the matrix are required. The biocomposites based on collagen with different inorganic fillers such as titania, hydroxyapatite, silica and layered silicates are well known for the healing of hard and soft connective tissue lesions [3-7]. In many cases, the matrices contain drugs, like antibiotics, which help the tissue regeneration and prevent the infection [8].

Matrixes covering other natural bioactive substances with antimicrobial and antioxidant effect, as methylene blue (MB) and quebracho (QBR), a tannin [10-16], were previously applied for medical purposes.

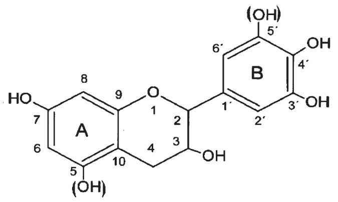

(1)

Previous modification of montmorillonite with QBR, having the general chemical structure depicted in formula 1, was done by Schott (1968) and by Freudenberg and Maitland (1934) and they showed that the tannin anions are adsorbed at the edge surfaces of the clay particles by complexing with the exposed octahedral aluminium ions. The basal spacing does not increase after tannin adsorption [9].

The methylene blue (MB) can be absorbed by the Na-montmorillonite as methylene blue cation ($MB^+$) [17, 18]. The amount of the adsorbed MB is influenced by the cationic exchange capacity (CEC) of the montmorillonite. In montmorillonite, at the beginning, there is a rapid adsorption on the external surfaces, followed by a slow interlayer cation exchange. This exchange depends on the accessibility of the large MB cation to the exchangeable cation. The cation replacement is not stoichiometric and the amounts increase with the dispersion degree of the clay. MB cations adjust the distribution of the layer charge, so that each cation could balance the charge due to one unequivalent substitution, eventualy reaching the chemical equilibrium [19].

Bergmann and O'Konskii (1963) studied the visible spectrum of MB adsorbed onto Na-montmorillonite. They observed four distinct adsorption bands around 575, 610, 670, and 760 nm (named $\gamma$-, $\beta$-, $\alpha$-, and J-bands, respectively) which were ascribed to high aggregates, dimers, monomers and the J band of the dimer, respectively [17].

The purpose of this work was to obtain nanocomposites by modifying the Valea Chioarului bentonite with an active substance (methylene blue, quebracho) and to dispers the hybrid into collagen gel in order to obtain biomaterials. The morphostructural properties and the biocompatibility of the collagen/ modified layered silicate nanocomposites are evaluated.

## Experimental part

### *Materials*

Sodium montmorillonite was obtained by purification of Romanian bentonite (BVC), with basal spacing $d_{001}$: 12.4 Å and 7% weight loss in the temperature range of 20÷120°C (TGA).

---

* *email: zvuluga@yahoo.com*

Collagen gel (COL) with average molecular weight 300000 Da, was extracted from bovine (calf) skin at the National Research and Development Institute for Textile and Leather – ICPI Division, Bucharest, Romania.

Methylene blue (MB) was purchased from Fluka and was used as received.

Quebracho (QBR) has been imported from Argentina by INCDTP-ICPI and was used as received.

### *Procedures*

### Sodium montmorillonite modification with active substances

- Sodium montmorillonite modification with methylene blue (BVC-MB)

The silicate surface modification with MB was performed by cationic exchange reaction, in 1:1 ethanol/ water mixture, at three BVC/MB ratios (2:1; 1:1 and 1:2).

The silicate was prior swelled 1% in distilled water over the night. The methylene blue was dissolved in 1:1 ethanol/ water mixture and mixed with the silicate suspension by a magnetic stirrer, at 70°C, 10 min. After 72 h, at 70°C in an oven with air circulation, the mixture was centrifuge-separated. The sediment was washed three times with hot water in order to remove the $Cl^-$ anions. The sediments were dried at 70°C, for 24 h.

- Sodium montmorillonite modification with quebracho (BVC-QBR)

QBR was dissolved in water, then, three mixtures of BVC/MB were prepared in 1:2, 1:1 and 2:1 ratios. The mixtures were kept at 70°C in an oven with air circulation. After 24 h the mixtures were separated and the sediments were dried at 70°C, for 24 h.

### Nanocomposites casting

Intercalated nanocomposites with disordered lamellar structure were obtained by uniform dispersing of the surface modified montmorillonite in a collagen gel, containing 1.1% dry substance. These compositions were cast in form of membranes (films) then dryed for 48 h at room temperature.

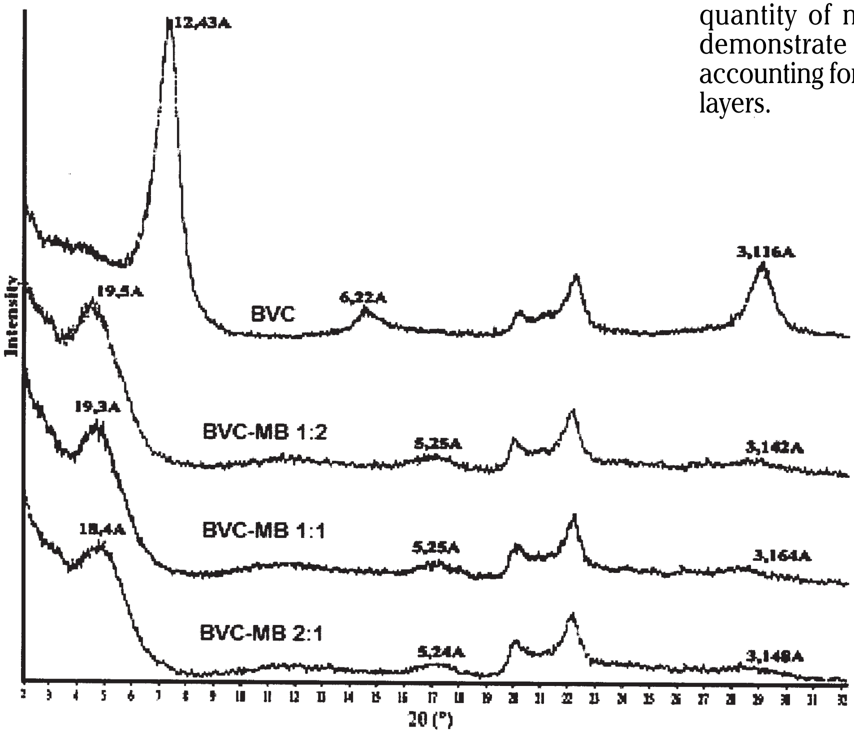

Fig. 1 X-ray diffraction patterns for the silicates modified with different ratios of MB vs. BVC

### Characterization

The basal spacing, $d_{001}$, was determined from X-ray diffraction (XRD) on a DRON goniometer; using the $CuK_\alpha$ radiation source ($\lambda$ = 1.5418 Å) filtered with Ni for $K_\beta$ component removing, in Bragg-Brentano system (by reflection); the patterns were automatically recorded at small angles (2θ: 2÷30°).

The weight losses of the surface modified silicates were determined by thermal gravimetric analysis (TGA), performed on a Thermal Analysis 2100 Du Pont system at the 20°C/min heating rate, in air. The temperature at the maximum rate of weight loss, on the second decomposition step, was determined from DTA curves.

Nanocomposites thermal analyses were done on a Netzsch DSC-TGA type STA 449 C-Jupiter, with 10°C/min, heating rate, under a current of He of $25cm^3$/min and in the 30-750°C temperature range.

Interaction between components was investigated through infrared spectroscopy (FTIR) using a Bruker VERTEX 70 spectrometer, with an ATR-HARRICK MVP2 diamond device in the range 4500-500 $cm^{-1}$ (folowing the procedure earlier described [20]) and through UV-Vis spectrophotometry on a Nicollet Evolution 500 instrument.

The shape and the size of the nanoparticles were observed by SEM images with an environmental scanning electron microscope EFI Quanta 200 instrument. The samples were nonconductive dry powders, recorded without metallisation, using the “low vacuum” mode (pressure 10-130 Pa).

Water vapor adsorption was determined in accordance to SR-5048/2:1999.The biocompatibility tests were done “in vitro” in fibroblast cell cultures.

## Results and discussion

### *Sodium montmorillonite modification with active substances*

### Sodium montmorillonite modification with methylene blue (BVC-MB)

The adsorption degree of methylene blue was revealed by X-ray diffraction, UV spectroscopy and thermo-gravimetric analysis.

From X-ray diffractions (fig. 1) it can be observed that, compared to BVC, in nanohybrids the peaks become broader, less intense and are shifted to lower angles as the quantity of methylene blue increases. These results demonstrate the increase of basal spacing by 6 - 7Å, accounting for the intercalation of the MB between silicate layers.

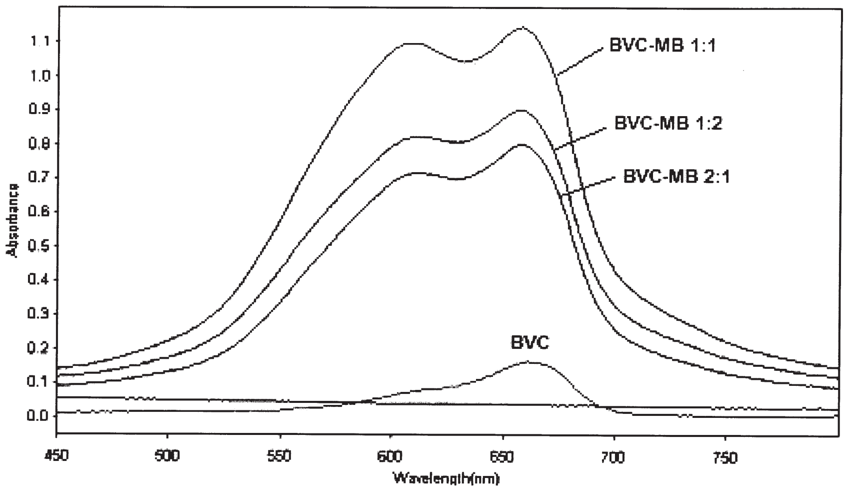

Fig. 2 UV adsorption for the silicates modified with different ratios of MB vs. BVC and MB

The visible light adsorption spectra correlate with the adsorbed MB quantity. Methylene blue adsorbs either in form of monomer and as dimer. In figure 2, peaks at 612 nm corresponding to the dimer of the methylene blue and at 658 nm corresponding to the methylene blue monomer can be observed. The adsorbance due to the two forms diminishes proportional with the increase of adsorbed MB quantity. It also can be observed that as the concentration of silicate increases the formation of the dimer is favored.

The results obtained by TGA (table 1) show that the binary hybrids exhibit enhanced thermal stability compared with the MB. In the range of the used temperature (20 - 700°C), the resulted products exhibit three main endothermic effects, same as MB. For bentonite, the first step of decomposition is in the temperature range of 20 - 200°C and represents the loss of residual water from silicate. The quantity of water loss is smaller in the binary hybrids. The temperature for the loss of residual water has similar values with those for bentonite (71 - 72°C), in the case of nanohybrids BVC-MB 2:1 and BVC-MB 1:2 and has higher values (approximately 160°C) for the nanohybrid BVC-MB 1:1. For this last sample, the mass loss at the maximum decomposition rate is at higher temperature (668°C), probably because of the increased interaction between BVC and MB at 1:1 ratio. The excess of BVC (in the case of nanohybrids BVC-MB 2:1) or MB (in the case of nanohybrids BVC-MB 1:2) induces an early decomposition of the entire material as can be seen from the temperatures of the maximum decomposition rate of the first step mentioned above. In this step the main process is dehydration of the material, starting at room temperature, therefore the onset of the decomposition is obscured and the temperatures of the maximum decomposition rate are used for comparison.

A proof that MB is intercalated between the silicate layers is the appearance of weight loss steps in the range 200 - 500°C, where the TG of bentonite is flat (fig. 3).

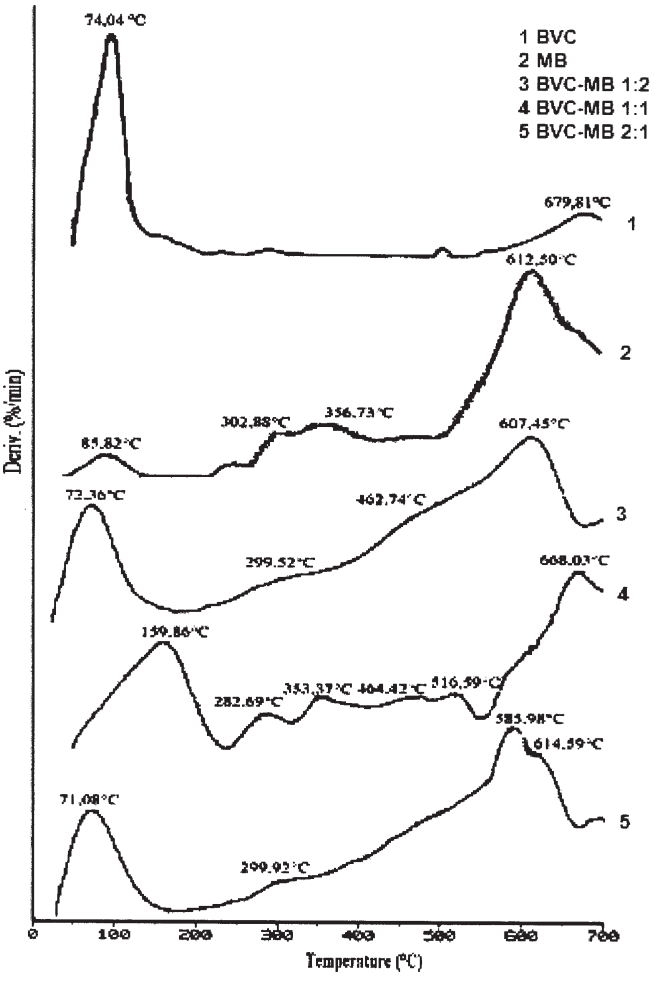

Fig. 3 Thermal stability for the silicates modified with different ratios of MB vs. BVC and MB

**Table 1**

TGA RESULTS FOR BVC INITIAL AND AFTER MODIFICATION WITH DIFFERENT RATIOS OF MB

| No. crt. | Sample | $T_{vd}$ (°C) | $R_{700}$ (%) | Mass loss on decomposition steps (%) | | |
|---|---|---|---|---|---|---|
| | | | | Step I (20°C-200°C) | Step II (200°C-500°C) | Step III (500-700°C) |
| 1 | BVC | 74 | 90.3 | 8.3 | - | 1.4 |
| 2 | MB | 612 | 27.7 | 1.6 | 18.3 | 52.4 |
| 3 | BVC-MB 1:2 | 607 | 78.5 | 2.7 | 8.8 | 10 |
| 4 | BVC-MB 1:1 | 668 | 90 | 2.4 | 2.9 | 4.7 |
| 5 | BVC-MB 2:1 | 586 | 80.7 | 2.6 | 8.3 | 8.4 |

Note:

$T_{vd}$: The temperature at the maximum rate of decomposition;

$R_{700}$: The residue at 700 °C.

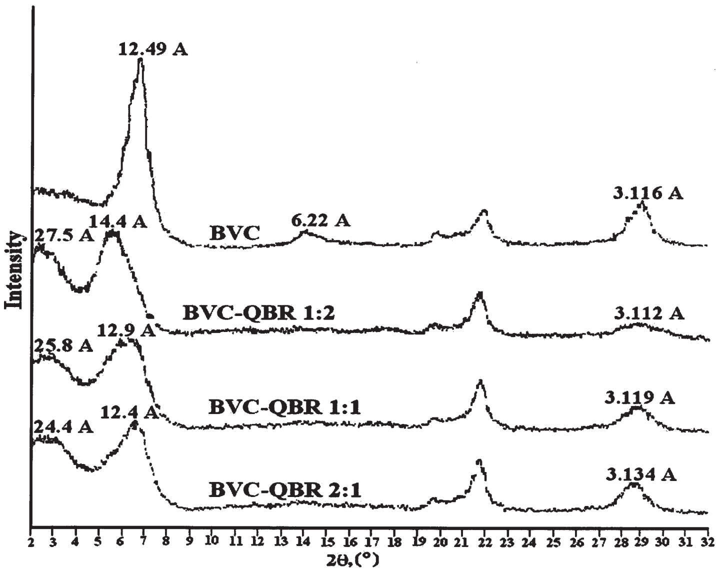

Fig. 4 X-ray diffraction patterns for the silicates modified with different ratios of QBR vs. BVC

*Sodium montmorillonite modification with quebracho (BVC-QBR)*

From X-ray diffractions presented in figure 4 it can be observed that, compared to BVC, in nanohybrids the peaks become broader, less intense and are shifted to lower angles, proving the formation of intercalated hybrids with disordered lamellar structure. The interlamellar distance slowly increases proportional with the increasing of quebracho content. This behaviour is the proof of polyphenol interaction with bentonite surface and probably the formation of a complex between the quebracho anions and the octahedral aluminium cations. Still, an ordered structure is retained in the hybrid bentonite/quebracho 1:1 ratio since two diffraction peaks may be observed – the diffraction peak at $2\theta \approx 3°$, and its harmonic at $2\theta \approx 7°$.

The TGA results (fig. 5) demonstrate that the modified bentonite with quebracho exhibits similar behaviour with the hydrophilic bentonite. For nanohybrids, the maximum weight loss rate is situated on the first step of decomposition, similar to bentonite. An enlargement of the decomposition range may be observed and a shifting of maximum decomposition rate to higher temperatures, proportional with the increase of quebracho content. As compared to purified bentonite which in the temperature range of 200-550°C is stable (does not decompose), nanohybrids show various decomposition steps, similar to those of quebracho, proving the interaction between bentonite and quebracho.

In the table 2 the weight loss on each step of decomposition is shown.

The low rate for the secondary peak at about 400°C proves the limited intercalation of quebracho between bentonite layers. These results are sustained by the above discussed X-ray diffraction patterns in figure 4.

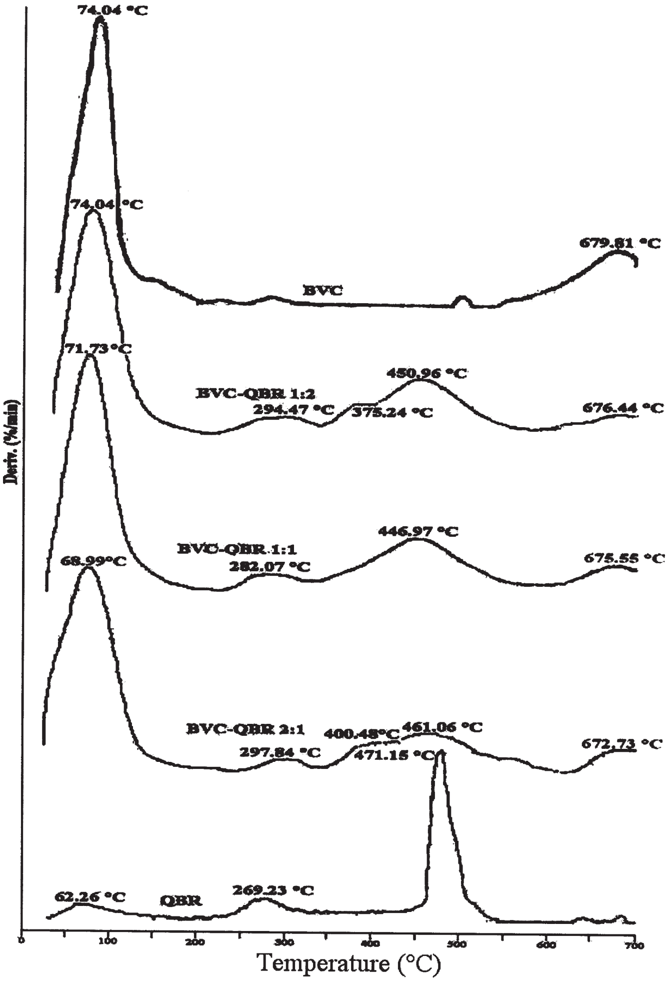

Fig. 5 DTA results for the silicates modified with different ratios of QBR vs. BVC and QBR

**Table 2**

WEIGHT LOSS FOR THE SILICATES MODIFIED WITH DIFFERENT RATIOS OF QBR COMPARED TO BVC AND QBR

| No. crt. | Sample | $T_{vd}$ (°C) | $R_{700}$ (%) | Mass loss on decomposition steps (%) | | |
|---|---|---|---|---|---|---|
| | | | | Step I (20°C-200 °C) | Step II (200°C-550 °C) | Step III (550°C-700 °C) |
| 1 | BVC | 74 | 90.3 | 8.3 | - | 1.4 |
| 2 | QBR | 471 | 10.7 | 9.4 | 77.9 | 2 |
| 3 | BVC-QBR 1:2 | 74 | 85.6 | 6.5 | 6.2 | 1.7 |
| 4 | BVC-QBR 1:1 | 72 | 86.5 | 6.4 | 3.1 | 4 |
| 5 | BVC-QBR 2:1 | 69 | 89 | 6 | 1.5 | 3.5 |

Note:

$T_{vd}$: The temperature at the maximum rate of decomposition;
$R_{700}$: The residue at 700 °C.

*Collagen based nanocomposite*

The X-ray diffraction patterns (fig. 6) reveal the interaction of the collagen with the bentonite. The specific peack of collagen (at $2\theta \approx 21°$), the shifting of the characteristic peak of bentonite towards small angles and the flattening of the silicate peak can be noticed in figure 6, proving the formation of nanocomposites with lamellar disordered structure (the diffraction peaks with greater breadths and lower intensities suggests a disorder in the stacking of the organosilicate layers [21]) either for the membranes with methylene blue or with quebracho.

The TGA results (fig. 7) show improved thermooxidative stability for nanocomposites based on collagen and Na montmorillonite modified either with quebracho or methylene blue compared to collagen membrane. In the range 20-700°C the samples show four endothermic effects, presented at lower temperatures in the case of collagen membrane. Collagen membrane decomposes with the maximum rate over 167°C compared with nanocomposite membranes which decompose with the maximum rate over 228°C. DSC curves show that nanocomposites decompose first endotermically then exothermically as compared to collagen membrane decomposing endothermically only.

The IR spectrum of collagen composite membrane presents the characteristic doublet for peptidic carbonyl at 1626 and 1591 cm$^{-1}$; the signal at 1626 cm$^{-1}$ has a low intensity due to interchain hydrogen bonds of carbonyl with –NH- group as it can be seen in figure 8.

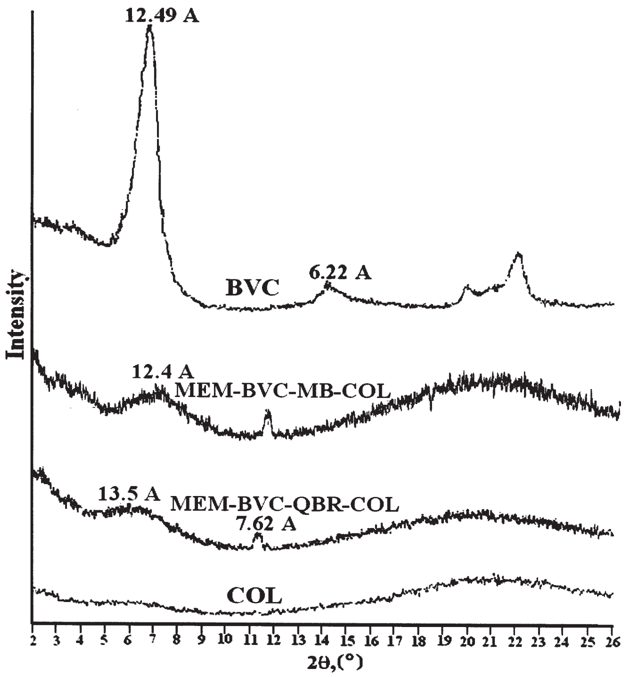

Fig. 6 X-ray diffraction patterns for collagen/ modified layered silicate nanocomposites

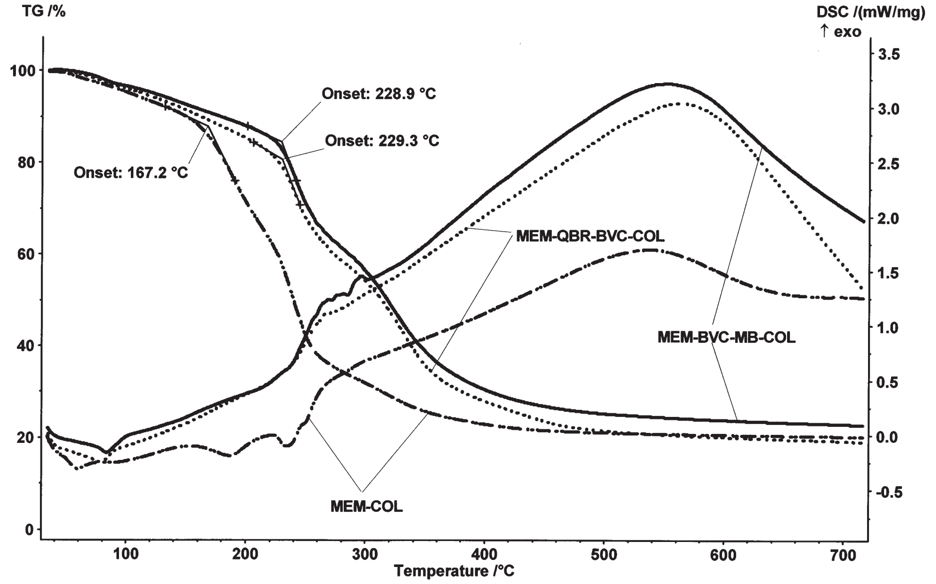

Fig. 7 DSC-TGA for nanocomposite membranes with quebracho and methylene blue vs. collagen membrane

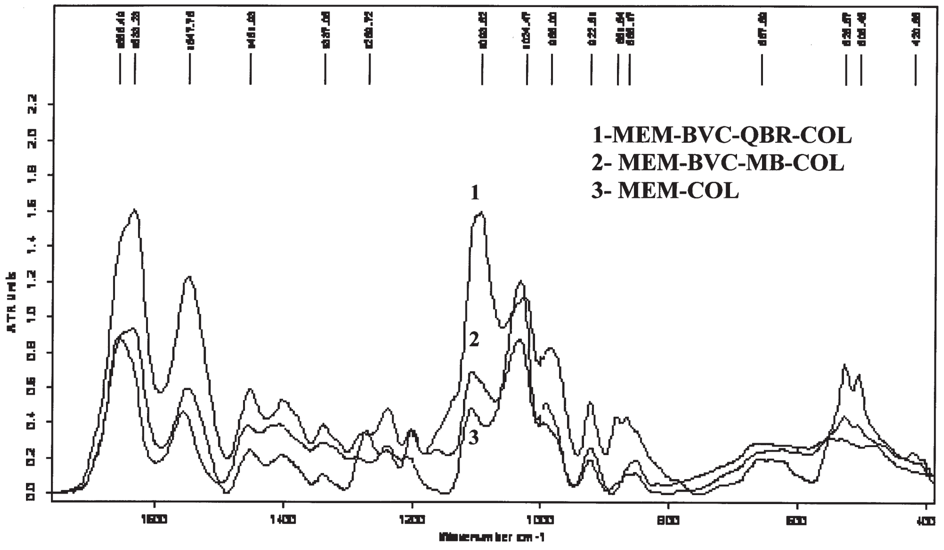

Fig. 8 FTIR for nanocomposite membranes with quebracho and methylene blue vs. collagen membrane in the range 400-1800 cm$^{-1}$

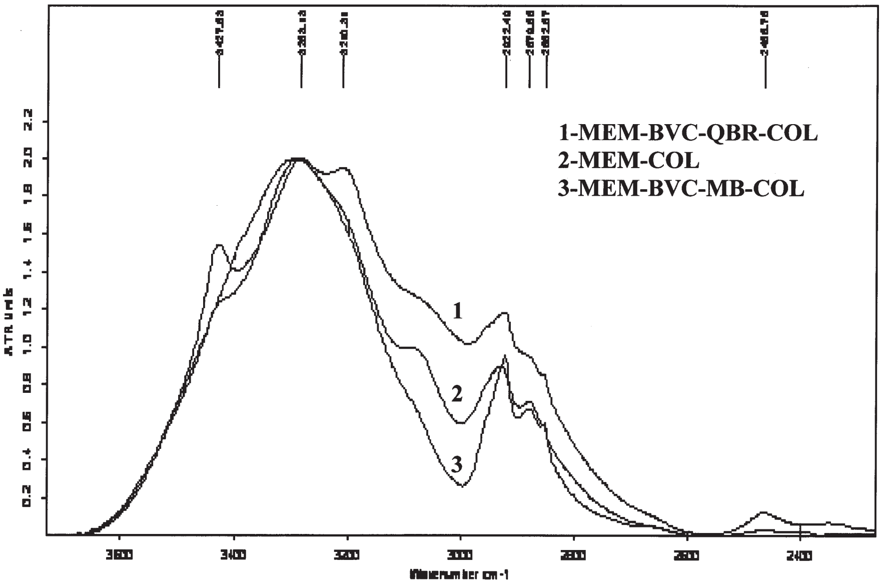

Fig. 9 FTIR for nanocomposite membranes with quebracho and methylene blue vs. collagen membrane in the range 2300-3800 cm$^{-1}$

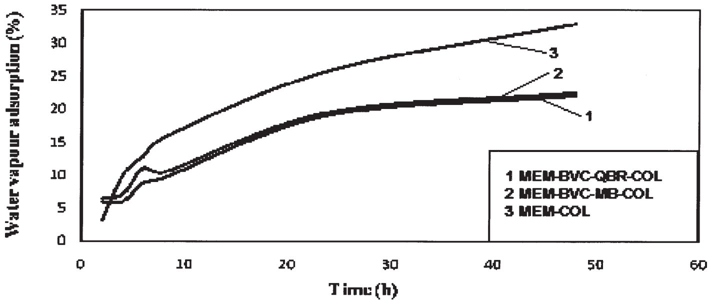

Fig. 10 Water vapour adsorption for nanocomposite membranes with quebracho and methylene blue compared with collagen membrane

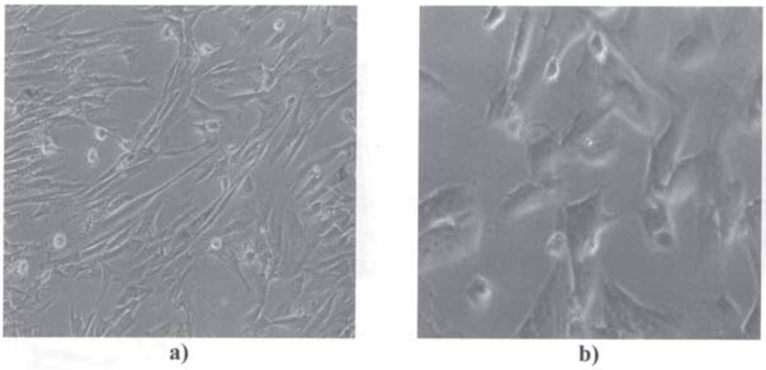
a) b)

Fig. 11 Biocompatibility for methylene blue membrane

a) after 24 h; b) after 72 h

In modified collagen this doublet presents a drastic modification due to interruption of interchain hydrogen bonds by additives. The signal at 1626 cm$^{-1}$ shows an increased intensity and the signal from 1591 cm$^{-1}$ shifts to 1549 cm$^{-1}$.

A similar effect may be observed in –NH region where the two distinct peaks from 3330 cm$^{-1}$ and 3128 cm$^{-1}$, corresponding to free and associate –NH from collagen, are merging in a centred broad band at 3300 cm$^{-1}$, corresponding to free and associated species with small molecular compounds (fig. 9) in fast exchange.

This phenomenon is obvious for both methylene blue and quebracho membranes.

From water vapour adsorption curves (fig. 10) it can be observed that the collagen membrane presents a continuous increasing variation on the whole time of exposure and a final adsorption after 48 h higher than in the case of nanocomposite membranes with quebracho and methylene blue. (around 35% compared to 20%). The membranes with modified silicate continuously adsorb water vapours in the first 24 h of exposure then reach a plateau (the adsorption remain almost constant in time).

The biocompatibility was tested on nanocomposite membranes "*in vitro*" on cellular cultures and was followed under a microscope in phase contrast equipped with a digital camera after 24 and 72 h respectively (fig. 11 and 12). The results show a good compatibility with human dermal fibroblast cells, the main type of cells from derma. The cells presented a normal phenotype and were uniformly distributed after 24 h as it can be seen in the figures 11 and 12. In case of the sample with methylene blue in the culture medium some blue deposits were observed, coming from the structure of the membrane which contains methylene blue.

After 72 h in the case of sample with methylene blue some phenotype cellular modification appeared as can be observed in the figure 11 b). The sample with quebracho presented a normal phenotype and the cells were uniformly distributed (fig. 12).

After 72 h from insemination the 3-(4,5-dimethyltiazol-2-il)-2,5-diphenyltetrazoliu (MTT) test was performed in order to test the cells viability.

Taking into account the MTT test, the cells viability for the quebracho membrane was 99% as compared to methylene blue membrane which presented a cells viability of only 30% after 72 h (table 3).

The obtained results are also confirmed by SEM images (fig. 13) from which the uniform dispersion of bentonite into collagen matrix and the interaction between them. A

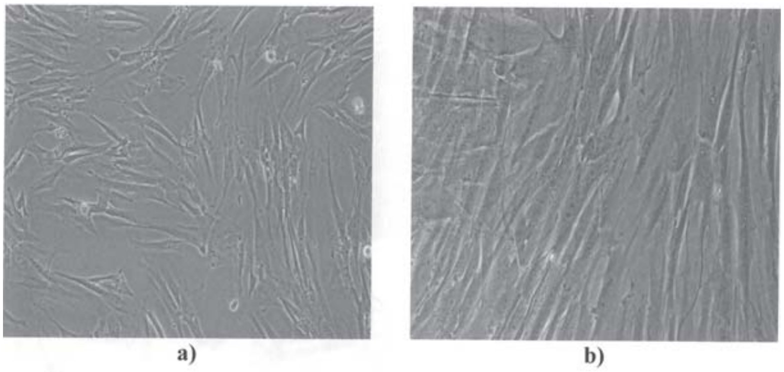
a) b)

Fig. 12 Biocompatibility for quebracho membrane
a) after 24 h; b) after 72 h

**Table 3**
CELLS VIABILITY FROM MTT TEST

| Sample | Optical density DO 550 nm | %Viability from control |
|---|---|---|
| Control | 0.6681 | 100% |
| MEM-BVC-AM-COL | 0.2058 | 30% |
| MEM-BVC-QBR-COL | 0.6613 | 99% |

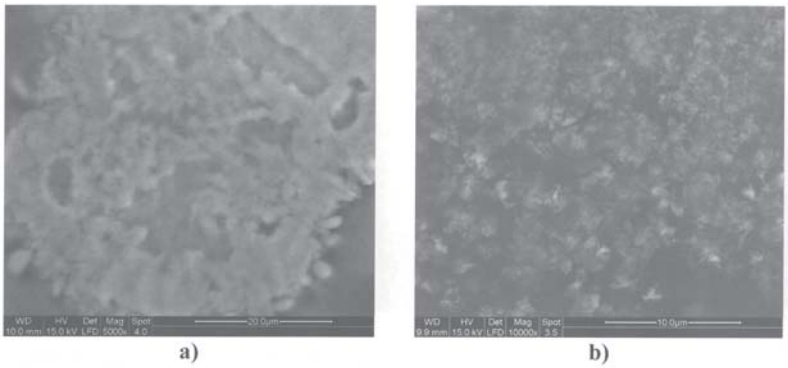
a) b)

Fig. 13 SEM images for nanocomposite membranes with
a) quebracho and b) methylene blue

better dispersion can be observed in the case of methylene blue nanocomposite. In the case of quebracho nanocomposite the tendency of agglomeration may be observed.

## Conclusions

Nanohybrides with lamellar disordered structure were obtained by modifying the layered silicate with quebracho and methylene blue. A better organization was observed in the structure of bentonite/quebracho 1:1 ratio.

TGA and XRD analyses proved the intercalation of active substances between the silicate layers. Thermal stability of the binary nanohybrides decreases with the increase of active substance content. Nanocomposites showed an improved thermal stability compared to collagen.

Modifying the silicate with active substances influences the hydrophilicity of final nanocomposite by reducing the water vapour adsorption.

Although the methylene blue is a disinfectant, it negatively influences the growth and development of the fibroblasts hence it is inappropriate for use in case of an open lesion.

Quebracho is biocompatible and has a biostimulating effect on the growth and development of the fibroblasts, bioactive films thus obtained being good antiseptic and regenerating patches.

*Aknowledgements: This work was achieved by means of the project PN2 CNMP Parteneriate 71-029 "Nabieco", financed by the Romanian Ministry of Education and Research.*

## References

1. VULUGA, Z., DONESCU, D., TRANDAFIR,V., RADOVICI, C., ŞERBAN, S., Rev.Roum.Chim., **52**, nr.4, 2007, p.395.
2. VULUGA, Z., DANCIU, V., TRANDAFIR, V., RADOVICI, C., VULUGA, D.M., ŞERBAN, S., POTÂRNICHE, C.G., Mol.Cryst.Liq.Cryst. **483**, 2008, p.258.
3. ITOH, S., KIKUCHI, M., KOYAMA, Y., TAKAKUDA, K., SHINOMIYA, K., TANAKA, J., Biomaterials, **23**, 2002, p.3919.
4. BONFIELD, W., J. Biomed. Eng., 10, 1988, p.522.
5. WANG, Y., UEMURA, T., DONG, J., KOJIMA, H., TANAKA, J., TATEISHI, T., Tissue Engineering, **9**, nr.6, 2003, p.1205.
6. MIYATA, N., FUKE, K.I., CHEN, Q., KAWASHITA, M., KOKUBO, T., NAKAMURA, T., Biomaterials, **25**, 2004, p.1.
7. FICAI, A., ANDRONESCU, E., GHIŢULICĂ, C., VOICU, G., TRANDAFIR, V., MÂNZU, D., FICAI, M., PALL, S., Mat. Plast., **46**, no. 1, 2007, p.11
8. SIAPI, E., MAVROMOUSTAKOS, T., TRANDAFIR, V., ALBU, G.M., Thermochimica Acta, **425**, 2005, p.165.
9. ULTRACKI, L.A., "Clay containing polymeric nanocomposites", Rapra Technology Limited, Shrewsbury, UK, **2004.**
10. MEISSNER, PE., MANDI, G., COULIBALY, B., *et al.,* Malaria Journal, **5**, 2006, p.84.
11. BROOKS, M.M., The Scientific Monthly, **43**(6), 1936, p.585.
12. LIN, LU., SHU-WEN, L., SHI-BO, J., SHU-GUANG ,W., Acta Pharmacol Sin, **25**, nr.2, 2004, p.213.
13. AKIYAMA, H., KAZUYASU, F., YAMASAKI, O., OONO, T., IWATSUKI, K., Journal of antimicrobial chemotherapy, **48**, 2001, p.487.
14. KOLODZIEJ, H., KIDERLEN, A.F., Phytochemistry, **66**, 2005, p.2056.
15. YANG, L.L., LEE, C.Y., YEN, K.Y., Cancer Letters, **157**, 2000, p.65.
16. CHEVALLIER, A., "Encyclopedia of Medicinal Plants", Dorling Kindersley, London, 1996
17. YARIV, S., CROSS, H., "Organo-clay complexes and interactions", Marcel Dekker, Inc., New York, 2002
18. HANG, P.T. BRINDLEY, G.W., Clays and Clay Minerals, **18**, 1970, p.203.
19. BUJDÁK, J., IYI, N., FUJITA, T., Clay Minerals, **37**, 2002, p.121.
20. VULUGA, DM., PANŢÎRU, M., HAMAIDE, T., VASILESCU, DS., Polymer Bulletin, **52**, 2004, p.349.
21. HOFFMANN, B., DIETRICH, C., THOMANN, R., FRIEDRICH, C., MULHAUPT, R., Macromol. Rapid Commun., **21**, 2000, p.57

Manuscript received: 17.1.22009